

Anderson localization at the boundary of a two-dimensional topological superconductor

Daniil S. Antonenko,^{1,2} Eslam Khalaf,³ Pavel M. Ostrovsky,^{1,4} and Mikhail A. Skvortsov¹

¹*L. D. Landau Institute for Theoretical Physics, Chernogolovka 142432, Russia*

²*Department of Physics, Drexel University, Philadelphia, PA 19104, USA*

³*Department of Physics, Harvard University, Cambridge, MA 02138, USA*

⁴*Max-Planck-Institut für Festkörperforschung, 70569 Stuttgart, Germany*

(Dated: December 14, 2021)

A one-dimensional boundary of a two-dimensional topological superconductor can host a number of topologically protected chiral modes. Combining two topological superconductors with different topological indices, it is possible to achieve a situation when only a given number of channels (m) are topologically protected, while others are not and therefore are subject to Anderson localization in the presence of disorder. We study transport properties of such quasi-one-dimensional quantum wires with broken time-reversal and spin-rotational symmetries (class D) and we calculate the average conductance, its variance and the third cumulant, as well as the average shot noise power for arbitrary wire length, tracing a crossover from the diffusive Drude regime to the regime of strong localization where only m protected channels conduct. Our approach is based on the non-perturbative treatment of the non-linear supersymmetric sigma model of symmetry class D with two replicas developed in our recent publication [D. S. Antonenko *et al.*, Phys. Rev. B **102**, 195152 (2020)]. The presence of topologically protected modes results in the appearance of a topological Wess-Zumino-Witten term in the sigma-model action, which leads to additional subsidiary series of eigenstates of the transfer-matrix Hamiltonian. The developed formalism can be applied to study the interplay of Anderson localization and topological protection in quantum wires of other symmetry classes.

I. INTRODUCTION

Quantum localization is a fundamental phenomenon first introduced in the seminal paper by Anderson [1] over 60 years ago. Since then numerous types and forms of localization effects have been identified [2] ranging from the quantum Hall effect [3] along with other topological insulators and superconductors [4] to many-body localization physics of interacting systems [5]. It is now a common knowledge that disorder can dramatically change the nature of quasiparticle wavefunctions leading to exponential suppression of transport due to quantum interference. These effects are especially pronounced in low-dimensional systems, where quasiparticles have less volume to avoid impurity scattering. In particular, it has been argued by a general scaling analysis that localization is unavoidable in one-dimensional systems [6]. However, this statement in its general form is undermined by recent developments in the physics of topological systems [4]. It was demonstrated that one-dimensional conductors of certain symmetry can host topologically protected modes that evade localization as long as the symmetry is preserved in the presence of disorder [7–9]. Such topologically protected modes can coexist with usual unprotected modes, when only the latter are subject to localization [10]. In the present paper, we consider a particular model of a superconductor with both protected and unprotected conducting channels and study various transport characteristics in this mixed arrangement for a broad range of system lengths.

We study transport properties of the one-dimensional (1D) boundary states of a two-dimensional (2D) topological superconductor of symmetry class D (broken time-

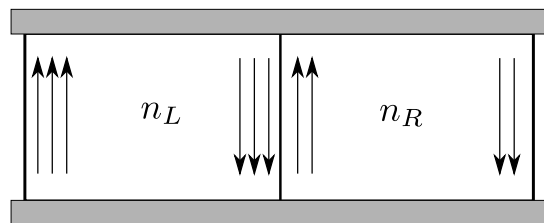


FIG. 1. Junction of two 2D topological superconductors as a possible experimental implementation of a quasi-1D system possessing $|n_R - n_L|$ protected modes and $\min\{n_L, n_R\}$ unprotected modes at the interface. Here n_L and n_R denote topological indexes of left and right superconductors, correspondingly. Terminals for transport measurements are shown by gray rectangles.

reversal and spin-rotational symmetries). According to the general classification [11, 12] of topological insulators and superconductors, in this symmetry class 2D bulk is characterized by a \mathbb{Z} topological index. Due to the bulk-boundary correspondence, the same index provides the number of topologically protected chiral edge states circulating around the boundary of the system. We consider a general setup with both protected and unprotected channels, which can be realized in a junction of two such 2D topological superconductors with different values of their topological indexes as shown in Fig. 1. This difference induces an imbalance between right- and left-propagating channels at the interface between superconductors thus leading to the coexistence of protected and unprotected modes [10].

Probing quasiparticle edge transport is a challenging task in a topological superconductor since electrical transport measurements are compromised by the shunting effect of the superconducting bulk. Spin of edge excitations is also not conserved due to the lack of spin-rotational symmetry making their spin conductance an ill-defined quantity. The only conserved physical property of the edge modes is their energy, hence it is only the *thermal conductance* that can reliably quantify edge transport. This is why topological effects in the superconductors of class D were dubbed as thermal quantum Hall effect (TQHE) [13]. We will characterize the edge modes by the value of their thermal conductance G_T and introduce a corresponding dimensionless conductance $g = G_T/G_0$, where $G_0 = \pi k_B^2 T/6\hbar$ is the quantum of thermal conductance [14]. To simplify the analysis, we will limit our consideration to the case of low temperatures and hence neglect possible inelastic scattering.

One particular way to controllably create a quasi-1D system with both protected and unprotected modes is bringing into contact two 2D topological superconductors with different topological indexes n_L and n_R as shown in Fig. 1. In this way, we obtain unequal numbers of left- and right-propagating modes at the interface. The difference $n_R - n_L$ gives the number of topologically protected modes that evade localization [10]. A similar setup was implemented experimentally for the quantum Hall physics (i.e. for a unitary symmetry class) in a 2D electron gas, located at a surface of a crystal with different filling factors on adjacent faces [15–18]. In our case of a topological superconductor, the topological classification and the geometry of protected edge states is the same.

In the setup of Fig. 1, the total conductance does not depend on the direction of the current between the terminals (denoted by gray rectangles). However, the current is distributed differently between the inner interface and outer edges depending on the overall current direction. Assume for a moment $n_L > n_R$. Then at the interface there are $m = n_L - n_R$ topologically protected modes propagating downwards. When a current flows from the upper to the lower terminal, it is carried by these modes together with n_R modes at the rightmost boundary. In total there are n_L protected modes and n_R unprotected channels carrying this current. In the opposite case when the current flows upwards it is carried by n_L protected modes on the leftmost edge of the system together with n_R unprotected channels at the interface in the middle. In the opposite case $n_L < n_R$ the argument is similar. Hence there are always $\max\{n_L, n_R\}$ protected and $\min\{n_L, n_R\}$ unprotected channels irrespective of the current direction. All unprotected modes are at the interface between superconductors while the number of protected modes at the same interface is $m = |n_L - n_R|$.

To simplify the analysis we find it convenient to consider direction-averaged dimensionless conductance of the interface g . We decompose the overall conductance g_{tot} into the contributions of outer edges and inner interface with both quantities averaged over the two possible

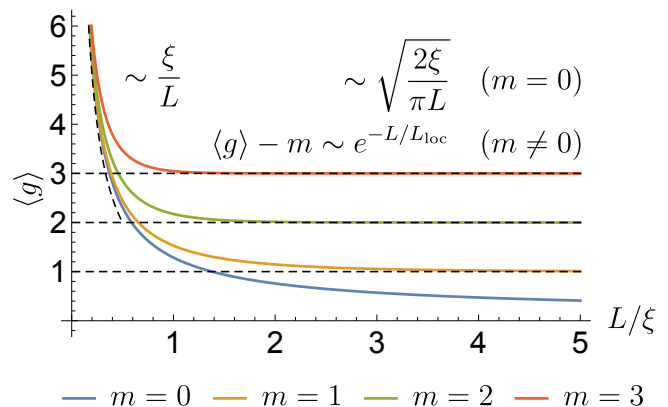


FIG. 2. Average conductance $\langle g \rangle$ in the presence of m protected topological modes as a function of the wire length L . Dashed lines show the leading short- and long-wire asymptotics. Localization length L_{loc} decreases with the increase of m according to Eq. (49).

directions of the current [10]:

$$g_{\text{tot}} = \frac{n_L + n_R}{2} + g. \quad (1)$$

Here the first term corresponds to the direction-averaged contribution of the outer edges of the junction (see Fig. 1). In the following we focus only on the second term g . We will study statistical properties of the interface conductance g , in particular, its averaged value $\langle g \rangle$, variance $\text{var } g$ and the third cumulant $\langle\langle g^3 \rangle\rangle$. Also, we will compute the shot noise power of quasiparticles which is also due to the channels at the interface.

The case without protected modes ($m = 0$, corresponding to $n_L = n_R$ in the aforementioned setup) is special and was extensively studied previously [8, 19, 20]. It can be implemented in a superconducting wire with broken time-reversal and spin-rotational symmetries and does not require an adjacent two-dimensional gapped bulk superconductor. Such systems have attracted a great interest in recent years both theoretically and experimentally since they are very promising candidates to realize Majorana bound states [21–23]. Gapped phases of such disordered wires are characterised by a one-dimensional \mathbb{Z}_2 topological index q , which takes only two possible values 0 or 1. This index distinguishes a trivial gapped state $q = 0$ and a topological state $q = 1$ that carries a pair of zero-energy Majorana states at the ends of the wire. Critical state between these two gapped phases is not fully localized by disorder [7–9, 24]. Instead it is characterized by subohmic scaling of the average conductance with the wire length $\langle g \rangle \propto 1/\sqrt{L}$.

In our previous publication [20], we computed conductance variance and other higher transport moments for a disordered Majorana wire with many conducting channels fine-tuned to the critical regime. In the present paper we extend our research taking into account possible topologically protected modes, which can appear only if

the studied 1D system is realized at an edge of a two-dimensional topological superconductor. Since such an edge model is gapless, the \mathbb{Z}_2 topological classification of Majorana wires does not apply in this case.

We use the formalism of the supersymmetric nonlinear sigma model [25], which is applicable to disordered systems in the diffusive regime at moderately short lengths. In a 1D geometry this implies a large number of conducting modes $n_{L,R} \gg 1$.

While the symmetry class of the sigma model is determined by the symmetry of the underlying system, the rank of the model depends on the particular averaged quantity to be studied. The simplest quantities such as the average density of states or conductance involve at most two Green functions (retarded and advanced). They can be calculated within the minimal sigma model of rank $n = 1$. Such analysis for a disordered 1D system of the symmetry class D was carried out both in the topologically trivial ($m = 0$) [8, 26–28] and topologically nontrivial ($m \neq 0$) [10, 29] settings. In the latter case, inclusion of the channel imbalance results in the appearance of a topological Wess-Zumino-Witten (WZW) term in the sigma-model action, with the coefficient proportional to $m = |n_L - n_R|$.

Minimal one-replica sigma model of class D allows to calculate only the average conductance $\langle g \rangle$. Higher moments of transport, such as conductance variance or shot noise power require averaging of more than two Green functions. Hence the sigma model with at least $n = 2$ replicas is required. Such a model was developed in our earlier work [20] for the topologically trivial wires with $m = 0$. In the present paper we generalize these model to include possible topologically protected modes in the case $m \neq 0$. Using this generalized model we will calculate the first three moments of the conductance as well as the average Fano factor for the shot noise.

Anticipating detailed discussion of our results in Secs. V and VI, in Fig. 2 we present the average conductance of a 1D system with m topologically protected modes as a function of the wire length L . It shows how the classical ohmic behaviour $\langle g \rangle \sim \xi/L$ at short lengths (ξ is an analogue of the localization length) undergoes a crossover to the regime where all unprotected modes are fully localized. In the limit $L \gg \xi$ conductance approaches the value $\langle g \rangle = m$ since only topologically protected modes evade Anderson localization. Fig. 2 demonstrates that the localization length of unprotected modes ξ decreases with increasing m .

The main technical achievement of this paper is the construction of the full set of eigenfunctions for the transfer-matrix Hamiltonian of the two-replica supersymmetric sigma model with the WZW term. This technique is closely connected with the Fourier analysis on the corresponding symmetric superspace (sigma-model manifold). In our previous work [20], we have constructed a full set of eigenstates of the Laplace operator on this superspace. This set has a complex hierarchical structure with some parts inherited from the one-replica model. In

the present paper, we generalize this construction to the $m \neq 0$ case, which results in a vector potential in the transfer-matrix Hamiltonian corresponding to the WZW term in the action. We will demonstrate that this vector potential gives rise to additional eigenfunctions corresponding to bound states on the supermanifold.

The paper is organized as follows. In Sec. II we introduce the sigma model formalism in application to the two-replica version of class D and present the calculation scheme for the transport moments. We briefly outline the algorithm described in detail in Ref. 20 and explain the modifications introduced by the WZW term. In Sec. III we construct the radial eigenbasis of the Laplace operator on the sigma-model supermanifold and discuss its differences compared to the $m = 0$ case. We use the constructed eigenfunctions to build the heat kernel of the sigma model in Sec. IV and comment on the integration peculiarities in the momentum space. We present results of our study in Sec. V and draw conclusions in Sec. VI. Details of the gauge factor calculation for the vector potential induced by the WZW term are given in Appendix.

II. SIGMA MODEL FORMALISM

In this Section we introduce the nonlinear sigma-model formalism and apply it to the calculation of the transport properties. In many aspects our analysis follows the simpler $m = 0$ case (disordered wire without protected modes) hence we refer the reader to Ref. [20] for the details of such a calculation. In the present Section we will particularly focus on the points that are specific for the topologically nontrivial $m \neq 0$ case.

A. Sigma-model with WZW term

We perform our study in the framework of the supersymmetric nonlinear sigma model [25]. Its objective is to average a product of a certain number n of bosonic and an equal number n of fermionic Green functions over disorder realizations. We call the parameter n the number of replicas in the theory. In a model of a superconducting symmetry class each Green function has an additional matrix structure in the Nambu-Gorkov space.

By extracting low-energy properties via functional integration approach, we arrive at an effective description of soft electronic modes of the disordered system (diffusons and cooperons) in terms of a field theory for a supermatrix field Q , which belongs to a certain supermanifold. In our case, the supermatrix $Q \in \text{BF} \otimes \text{N} \otimes \text{R}$ belongs to the tensor product of the Nambu-Gor'kov (N), Bose-Fermi (BF), and replica (R) spaces. Hence the overall size of Q is $4n$. In addition, Q satisfies $Q^2 = 1$ and is subject to the charge conjugation constraint $\bar{Q} = C^T Q^T C = -Q$. The latter reflects superconducting symmetry of the underlying Bogoliubov-de Gennes Hamiltonian. Matrix C , which defines charge

conjugation, should satisfy $C^T C = 1$ and $C^2 = -k$, where $k = \text{diag}\{1, -1\}_{\text{BF}}$ is a signature matrix in the BF space. In general, the matrix Q can be represented as

$$Q = T^{-1} \Lambda T, \quad \bar{T} = T^{-1}. \quad (2)$$

The matrix Λ represents a certain point on the sigma-model manifold satisfying $\bar{\Lambda} = -\Lambda$, $\text{str} \Lambda = 0$, and $\Lambda^2 = 1$. The whole manifold is then generated by rotations of Λ with elements T from the corresponding supergroup G . Within G there are certain rotations that commute with Λ and hence do not change Q . They form a subgroup $K \subset G$. The sigma-model manifold is thus a *symmetric superspace* (coset) G/K with $[K, \Lambda] = 0$.

The sigma-model action for the quasi-1D topological wire of symmetry class D has the form [10]

$$S = - \int_0^L dx \left[\frac{\xi}{16} \text{str}(\nabla Q)^2 + \frac{m}{2} T^{-1} \Lambda \nabla T \right]. \quad (3)$$

Here $\xi = (n_L + n_R)l$ is the correlation length and l is the mean free path. The second Wess-Zumino-Witten (WZW) term in the action takes into account the imbalance between right- and left-propagating channels. Its prefactor $m = |n_R - n_L|$ determines the number of topologically protected modes in the system.

The WZW term in the action (3) is written in terms of the matrix T rather than Q . However, due to the peculiarity of the WZW term, the action evaluated on closed trajectories depends only on the Q -matrix configuration. To see this, consider a transformation $T \mapsto UT$, where $U \in K$ and thus $[U, \Lambda] = 0$. Such a gauge transformation changes T but leaves Q invariant. The corresponding change of the action is

$$\begin{aligned} T &\mapsto UT, & [U, \Lambda] &= 0, \\ S &\mapsto S - \frac{m}{2} \int_0^L \text{str} U^{-1} \Lambda \nabla U. \end{aligned} \quad (4)$$

The property $[U, \Lambda] = 0$ allows us to express the change in the action as a total derivative:

$$\text{str} U^{-1} \Lambda \nabla U = \text{str} \Lambda \nabla \log U. \quad (5)$$

Assume that the freedom of gauge choice is somehow fixed [see Eqs. (17) and (21) below]. That is, to every value of Q we assign a certain unique value of T . Then a closed trajectory in terms of Q is automatically closed also in terms of T . If the transformation $T \mapsto UT$ preserves this condition, matrix U should also follow a closed trajectory in the group K . Hence the integral of the total derivative (5) takes only integer values in units $4\pi i$. Since the topological index m itself takes only integer values, the statistical weight e^{-S} appears to be well-defined.

For a supersymmetric sigma model of class D with n replicas, the target manifold is $\text{SpO}(n, n|2n)/\text{U}(n|n)$ [30]. Its compact fermi-fermi sector $\text{O}(2n)/\text{U}(n)$ has two disjoint components corresponding to the two components

of the $\text{O}(2n)$ group. Such a structure of the sigma-model manifold implies that the Q matrix configurations can include jumps between the two parts of the target manifold. Inclusion of such jumps is necessary to ensure proper exponential localization in wires of class D [8, 28, 31] without topological terms.

In our earlier work Ref. [20] we studied a critical regime between topological and trivial gapped states in a Majorana wire of class D. This problem corresponds to the case $m = 0$ and to the absence of jumps between two parts of the manifold. The latter condition is ensured by the fact that the statistical weight of such jumps changes sign at the transition between trivial and Majorana state [8]. In the present case of an imbalanced system with $m \neq 0$, the jumps of the matrix Q are also fully suppressed. Indeed, the WZW term introduces a random phase factor to the amplitude of every jump. Averaging over these phases completely cancels possible contribution of such discontinuous configurations of Q . This is quite natural since both in the critical regime with $m = 0$ studied earlier and for the topological edge transport with $m \neq 0$ considered here full localization does not occur. This means we can limit our study of the sigma model of class D only to the connected component of the manifold $\text{SO}(2n)/\text{U}(n)$ in the compact sector.

B. Cartan-Efetov parametrisation

All physical observables of a disordered system can be inferred from the partition function of the nonlinear sigma model. For a system of 1D geometry this partition function is given by the path integral with the sigma-model action. The symmetry of the sigma-model manifold always allows us to bring the initial point of any trajectory to Λ . Hence we consider only path integrals for trajectories starting at $Q = \Lambda$

$$Z[Q] = \int_{Q(0)=\Lambda}^{Q(L)=Q} \mathcal{D}[Q(x)] e^{-S[Q]}. \quad (6)$$

The end point of the path integral can be also brought to its simplest form by some rotation $Q \mapsto U^{-1} \Lambda U$ with $[\Lambda, U] = 0$. Such rotations with a constant matrix U do not shift the initial point and also preserve the form of the action. To take advantage of this symmetry we will use the Cartan decomposition of the group G and define Cartan-Efetov coordinates on the sigma-model manifold.

Any matrix $T \in G$ can be decomposed into the following product:

$$T = U_1 e^{\tilde{\theta}/2} U. \quad (7)$$

Both matrices U_1 and U commute with Λ and thus belong to the subgroup G while $\tilde{\theta}$ is taken from the maximal abelian subalgebra of group G whose generators anticommute with Λ : $\{\Lambda \tilde{\theta}\} = 0$. This representation is known as the Cartan decomposition of T and $\tilde{\theta}$ is an element of

the Cartan subalgebra. With such a form of the matrix T , we have

$$Q = U^{-1} \Lambda e^{\check{\theta}} U. \quad (8)$$

Matrix Q is independent of U_1 and belongs to the coset space G/K as was discussed above. We see that by a certain U rotation it is always possible to bring the final point of our path integral (6) to the form $Q = \Lambda e^{\check{\theta}}$. Hence the partition function depends on the Cartan angles $\check{\theta}$ only.

Since the Cartan subalgebra is abelian it is always possible to choose a representation that brings $\check{\theta}$ to explicitly diagonal form. In class D with $n = 2$ replicas there are two Cartan angles in the non-compact boson sector and only one angle in the compact fermion sector. We will denote these angles as θ_{B1} , θ_{B2} , and θ_F . Partition function 6 depends only on the values of these angles at the final point of all trajectories. Once the partition function is known we can readily express first three moments of conductance by the following derivatives [20]:

$$\langle g \rangle = -4 \left. \frac{\partial^2 Z(\theta_i)}{\partial \theta_{B1}^2} \right|_0, \quad (9a)$$

$$\langle g^2 \rangle = 16 \left. \frac{\partial^4 Z(\theta_i)}{\partial \theta_{B1}^2 \partial \theta_{B2}^2} \right|_0, \quad (9b)$$

$$\langle g^3 \rangle = -32 \left. \frac{\partial^6 Z(\theta_i)}{\partial \theta_{B1}^2 \partial \theta_{B2}^2 \partial \theta_F^2} \right|_0, \quad (9c)$$

Here every derivative is taken at the point $\check{\theta} = 0$.

Strictly speaking, in the evaluation of the partition function (6) we consider trajectories $Q(x)$ starting at Λ and ending at Q with certain non-zero values of the Cartan angles $\check{\theta}$. Such trajectories are not closed and the WZW term in the action is not well-defined for them as explained above. This issue can be resolved in the following way. We augment each trajectory going from Λ to Q with an additional segment that goes back from Q to Λ and makes the trajectory closed. The simplest choice is to take the shortest closing path along a geodesic line on the sigma-model manifold. We only need to add the value of the WZW term along this additional segment to the overall action. This procedure will naturally add the contribution of the outer edges of the sample in Fig. 1 to the transport characteristics of the sample. More detailed discussion of this closing procedure can be found in Ref. [10]. Nevertheless, in the following analysis we will omit this contribution of outer edges and focus on the transport along inner interface only.

The structure of the symmetric supermanifold of the sigma model can be further detailed by specifying the corresponding roots and root vectors. A general matrix T in the definition (2) can be chosen in the exponential form $T = e^W$ where $W = -\bar{W}$. Matrices W obey a linear constraints and thus span a certain linear space (Lie algebra of the group G). We construct a basis in this space by defining root vectors Z_α . They are simultaneous eigenvectors of the adjoint action of all elements of the Cartan

TABLE I. Root system for sigma-model manifold of class D with $n = 2$ replicas: positive roots (α), their multiplicities (m_α) and corresponding root vectors ($Z_{\alpha(i)}$). The matrix Ξ_{ij} has 1 at the position (i, j) and 0 elsewhere.

Bosonic ($m_\alpha = 1$)		Fermionic ($m_\alpha = -2$)		
α	Z_α	α	$Z_{\alpha,1}$	$Z_{\alpha,2}$
$2\theta_{B1}$	Ξ_{18}	$\theta_{B1} + i\theta_F$	$\Xi_{15} - \Xi_{38}$	$\Xi_{16} + \Xi_{48}$
$2\theta_{B2}$	Ξ_{27}	$\theta_{B1} - i\theta_F$	$\Xi_{13} - \Xi_{48}$	$\Xi_{14} + \Xi_{68}$
$2\theta_F$	$\Xi_{36} + \Xi_{45}$	$\theta_{B2} + i\theta_F$	$\Xi_{25} - \Xi_{37}$	$\Xi_{26} + \Xi_{47}$
$\theta_{B1} + \theta_{B2}$	$\Xi_{17} - \Xi_{28}$	$\theta_{B2} - i\theta_F$	$\Xi_{23} - \Xi_{57}$	$\Xi_{24} + \Xi_{67}$
$\theta_{B1} - \theta_{B2}$	$\Xi_{12} - \Xi_{78}$			

subalgebra: $[\check{\theta}, Z_\alpha] = \alpha(\check{\theta})Z_\alpha$. Indeed, since Cartan subalgebra is abelian, it is always possible to simultaneously diagonalize all the commutators $[\check{\theta}, \cdot]$ and find the basis of root vectors Z_α . The corresponding eigenvalue $\alpha(\check{\theta})$ is a linear function of all the elements of $\check{\theta}$. It is called a root and can be viewed as a vector from the conjugate space to the Cartan subalgebra. We will include in the basis $\{Z_\alpha\}$ only nonzero root vectors, that is we exclude the elements of Cartan subalgebra from this set. If a certain simultaneous eigenvalue $\alpha(\check{\theta})$ is degenerate and has more than one corresponding root vector Z_α , we say that the multiplicity m_α of this root is greater than one. In a supersymmetric space there are bosonic and fermionic roots. Fermionic roots have Grassmann-valued root vectors and their degeneracy is always at least 2. However, the corresponding multiplicity should be taken with a negative sign [32]: $m_\alpha = -2$.

Roots obey a set of remarkable geometrical properties that allows to fully classify all possible symmetric spaces by their root systems. However, this goes beyond the scope of our paper. In the following analysis we will only need the following simple property: if $\alpha(\check{\theta})$ is a root, $-\alpha(\check{\theta})$ is also a root. We can separate the full set of roots into two halves by drawing a hyperplane in the space of roots (conjugate to the Cartan subalgebra). All the roots that point to one side of this hyperplane are called positive roots; their set we will denote R^+ . The roots pointing in the other halfspace are called negative. For every positive root α there is always a corresponding negative root $-\alpha$.

It is always possible to represent matrices t that generate the rotation T such that the abelian Cartan subalgebra corresponds to diagonal matrices. Furthermore, it is also possible to bring the matrices representing all positive root vectors to explicitly upper triangular form. Then negative root vectors will be given by lower triangular matrices. We list roots and root vectors for the sigma-model manifold of symmetry class D with $n = 2$ replicas in Table I.

The knowledge of the root system gives us one important piece of information that will be extensively used below. Namely, it allows us to find a Jacobian of the

Cartan parametrization [33]:

$$J(\theta_i) = \prod_{\alpha \in R^+} \left[\sinh \frac{\alpha(\theta)}{2} \right]^{m_\alpha} \\ = \frac{(\cosh \theta_{B1} - \cosh \theta_{B2}) \sinh \theta_{B1} \sinh \theta_{B2} \sin \theta_F}{(\cosh \theta_{B1} - \cos \theta_F)^2 (\cosh \theta_{B2} - \cos \theta_F)^2}. \quad (10)$$

This Jacobian is the square root of the determinant of the metric tensor and hence defines the invariant integration measure in Cartan angles $\check{\theta}$.

C. Transfer-matrix approach

Evaluation of the partition function (6) can be accomplished within the transfer-matrix technique [34]. It amounts to mapping the path integral to the evolution operator of the corresponding quantum Hamiltonian in the imaginary time x . We can thus equate the partition function to the resulting wave function after the evolution

$$Z[\check{\theta}] = \psi(Q = \Lambda e^{\check{\theta}}, x = L). \quad (11)$$

The result of such an evolution is usually termed heat kernel. Changing of ψ with x is governed by the Schrödinger equation with the Hamiltonian derived from the action (3),

$$\frac{\xi}{2} \frac{\partial \psi(Q, x)}{\partial x} = -\hat{H} \psi(Q, x). \quad (12)$$

Initial condition is $\psi(Q, x = 0) = \delta(Q, \Lambda)$ with the delta function that fixes $Q = \Lambda$.

The heat kernel can then be expressed as the spectral decomposition over the eigenfunctions ϕ_ν of \hat{H} :

$$\psi(Q, x) = \sum_\nu \mu_\nu \phi_\nu(Q) e^{-2\epsilon_\nu x / \xi}, \quad (13)$$

where ϵ_ν are the eigenvalues and μ_ν is a proper measure.

In a given coordinate system X_α on the sigma-model manifold, the transfer-matrix Hamiltonian for the action (3) has the form [29]:

$$\hat{H} = -\frac{1}{J} (\partial_\alpha - A_\alpha) J g^{\alpha\beta} (\partial_\beta - A_\beta). \quad (14)$$

Here $g_{\alpha\beta}$ is the metric tensor for the related to the length element as [25, 29].

$$-\frac{1}{2} \text{str} dQ^2 = g_{\alpha\beta} dX^\alpha dX^\beta. \quad (15)$$

The factor $J = \sqrt{\text{sdet } g}$ is the Jacobian given in Eq. (10). A new ingredient here compared to the $m = 0$ case is the appearance of a vector potential A_α generated by the WZW term:

$$A_\alpha = \frac{m}{2} \text{str} T^{-1} \Lambda \partial_\alpha T. \quad (16)$$

As was already discussed earlier, this vector potential is written in terms of T rather than Q , and hence is not gauge invariant. Fixing the gauge means assigning a particular unique matrix T to every value of Q . This will allow to express A_α as a function of Q .

We will use the gauge

$$T = U^{-1} e^{\check{\theta}/2} U. \quad (17)$$

It means that we fix the matrix $U_1 = U^{-1}$ in the Cartan decomposition (7) of T . Substituting Eq. (17) into Eq. (16), it is easy to see that the vector potential depends on the Cartan angles $\check{\theta}$ only. This property will greatly simplify further analysis. Indeed, initial condition of the evolution $Q = \Lambda$ is invariant under rotations $Q \mapsto U^{-1} Q U$ with any matrix U that commutes with Λ . The same property is also ensured for the Hamiltonian (14) in the chosen gauge (17). Hence we can limit our consideration to the ‘‘radial’’ eigenfunctions ϕ_ν that depend only on $\check{\theta}$.

This situation is similar to solving quantum evolution problem for a charged particle on a 2D plane subject to a uniform magnetic field. If one chooses circular gauge with the origin that coincides with the initial position of the particle the whole evolution operator at all times will depend only on the radial coordinate but not on the polar angle.

We can write explicitly the radial Hamiltonian that involves only the Cartan angles $\check{\theta}$:

$$\hat{H} = -\Delta + W(\check{\theta}), \quad (18)$$

where the radial Laplace operator is

$$\Delta = \frac{1}{J} \left(\frac{\partial}{\partial \theta_{B1}} J \frac{\partial}{\partial \theta_{B1}} + \frac{\partial}{\partial \theta_{B2}} J \frac{\partial}{\partial \theta_{B2}} + \frac{1}{2} \frac{\partial}{\partial \theta_F} J \frac{\partial}{\partial \theta_F} \right) \quad (19)$$

and the Jacobian is given in Eq. (10).

A new ingredient of the Hamiltonian is the potential term $W(\check{\theta}) = -A_\alpha A^\alpha$ induced by the WZW term in the action (3). For the sigma model of class D with $n = 2$ replicas this potential is

$$W(\check{\theta}) = \frac{m^2}{4} \left(\tanh^2 \frac{\theta_{B1}}{2} + \tanh^2 \frac{\theta_{B2}}{2} + 2 \tanh^2 \frac{\theta_F}{2} \right). \quad (20)$$

In the next section we will explicitly construct eigenfunctions of the Hamiltonian (18).

D. Iwasawa parametrisation

Eigenfunctions of the radial Laplace operator (19) can be efficiently constructed by considering the full Laplace operator in Iwasawa coordinates [27, 32, 33]. This representation is based on the following decomposition of the matrix T :

$$T = V e^{\check{\theta}/2} N. \quad (21)$$

Here V is a matrix that commutes with Λ , \check{a} is an element of the Cartan subalgebra parametrized by three angles a_{B1} , a_{B2} , and a_F , and $N = e^n$ is an exponential of a nilpotent matrix n that represents a linear combination of positive root vectors.

It is known that in the $m = 0$ case this parametrization has the following important property. Radial Laplace operator in Iwasawa coordinates [part of the full Laplace operator (14) that involves only \check{a}] does not explicitly depend on \check{a} . Instead, it involves only derivatives with respect to \check{a} and hence simple plane waves $\exp(i \sum_i p_i a_i)$ are the radial eigenfunctions.

It turns out [29] that this property does persist in the presence of the WZW term when the proper gauge choice is made. Namely, one should assume $V = 1$ in the decomposition (21). Then the \check{a} -dependent part of the Hamiltonian takes the following simple form:

$$\hat{H} = - \left(\frac{\partial^2}{\partial a_{B1}^2} + \frac{\partial^2}{\partial a_{B2}^2} + \frac{1}{2} \frac{\partial^2}{\partial a_F^2} - \frac{\partial}{\partial a_{B2}} + \frac{i}{2} \frac{\partial}{\partial a_F} \right). \quad (22)$$

Radial Laplace operator in the Iwasawa coordinates is not only independent of \check{a} but also does not contain any potential whatsoever!

Eigenfunctions of the radial Hamiltonian (22) in Iwasawa coordinates are plane waves

$$\phi_q(\check{a}) = \exp \left[i q_1 a_{B1} + \left(i q_2 + \frac{1}{2} \right) a_{B2} + i \left(l - \frac{1}{2} \right) a_F \right]. \quad (23)$$

Below we will also use a short-hand notation for this linear combination: $\phi_q(\check{a}) = e^{i q \cdot \check{a}}$. The corresponding eigenvalue for this plane wave is

$$\hat{H} \phi_q = \epsilon_q \phi_q, \quad \epsilon_q = q_1^2 + q_2^2 + \frac{l^2}{2} + \frac{1}{8}. \quad (24)$$

We have thus established a set of radial eigenfunctions in the Iwasawa coordinates. In order to calculate the heat kernel (13), we will need radial eigenfunctions in the Cartan-Efetov coordinates. Let us first relate the two sets of coordinates to each other:

$$T = V e^{\hat{a}/2} N = U^{-1} e^{\check{\theta}/2} U. \quad (25)$$

This matrix identity allows us to express \check{a} and V as functions of $\check{\theta}$ and U . In Ref. [20], we have discussed in detail how to resolve these equations for \check{a} . Solution for the matrix $V(\check{\theta}, U)$ is explained in Appendix. Let us note that we have chosen here T in the proper radial gauge (17) for the Cartan parametrization. However, this does not correspond to the proper gauge in Iwasawa coordinates since $V \neq 1$. We can account for this new gauge choice in the Iwasawa coordinates by multiplying the plane wave eigenfunction (23) with the proper phase factor:

$$\phi_q(\check{\theta}, U) = e^{-(m/2) \text{str} \Lambda V(\check{\theta}, U)} e^{i q \cdot \check{a}(\check{\theta}, U)}. \quad (26)$$

Further steps in the derivation of radial wave functions follow Refs. [20, 29]. By construction the new function (26) is automatically an eigenfunction of the full

Hamiltonian (14) in Cartan coordinates $\check{\theta}$ and U with the gauge (17). However, this eigenfunction does explicitly depend on U . In order to obtain the corresponding radial eigenfunction that depends on $\check{\theta}$ only, one has to perform *isotropization* of (26) over the group K of all possible matrices U :

$$\phi_q(\check{\theta}) = \left\langle e^{-(m/2) \text{str} \Lambda V(\check{\theta}, U)} e^{i q \cdot \check{a}(\check{\theta}, U)} \right\rangle_{U \in K} \quad (27)$$

Usually (for noncompact symmetric spaces) isotropization (27) is performed by integration over K group. However, as explained in detail in Ref. [20], the peculiarity of the supersymmetric model is that a naïve integration over the whole K group leads to the loss of some eigenfunctions. This happens because for certain values of momentum vector q the integrand lacks some of the Grassmann variables and the whole integral vanishes. A correct strategy to obtain these extra eigenfunctions is to integrate only over required Grassmann variables, which can be achieved by a special parametrization of the U matrix.

Isotropization over U in Eq. (27) can not be performed analytically. However, we can extract asymptotic expressions both in the large and small $\check{\theta}$ limit in the same way it was done in Ref. [20] for the case $m = 0$. This is sufficient to both normalize the radial wave functions and to extract derivatives required for the calculation of transport moments (9).

To identify domains of the momentum q that corresponds to normalizable wavefunctions, we can analyze asymptotic behavior of ϕ_q at large values of θ_{B1} and θ_{B2} . The function $\sqrt{J} \phi_q(\check{\theta})$ should not contain any exponentially growing terms. This condition will be automatically fulfilled if we choose real values of q_1 and q_2 specified in Eq. (23). It turns out that for a model with nonzero m some extra eigenstates emerge with discrete imaginary values of q_1 and/or q_2 . These eigenstates represent discrete localized levels in the potential (20). They will be discussed in detail in the next section. The third component of momentum l takes only integer values to ensure a regular single-valued form of the eigenfunction in the compact sector of the model. In the presence of the WZW term allowed values of l should be not less than m . This is a yet another effect of the potential term (20), which expels lowest eigenstates in the compact sector.

A generic radial eigenfunction is always invariant with respect to flipping the sign of any element of $\check{\theta}$ and also under the interchange of variables $\theta_{B1} \leftrightarrow \theta_{B2}$. This property follows from the fact that such transformations are equivalent to certain rotations $U \in K$. A similar symmetry is also present in momentum space: changing sign of any component of momentum or interchanging $q_1 \leftrightarrow q_2$ leaves the radial wave function invariant. This is a consequence of the Weyl group symmetry of the root system. Therefore we can limit the space of eigenfunctions to the domain $q_1 > q_2 > 0$ and to the positive values of l only. A similar property also applies to localized states in the noncompact sector that correspond to discrete imaginary

values of q_1 and q_2 . We will thoroughly discuss this topic in the next section.

III. STRUCTURE OF THE EIGENBASIS

In the $m = 0$ case [20], we found that the radial eigenbasis of the Laplace-Beltrami operator on the $n = 2$ sigma-model supermanifold has a hierarchical structure and consists of three subfamilies: (i) three-parametric subfamily, (ii) one-parametric subfamily, and (iii) the zero mode (just unity in that case). While the three-parametric subfamily is routinely obtained via the Iwasawa trick, identifying one-parametric subfamily and the zero mode following the same approach is a non-trivial task. It requires modification of the standard procedure to avoid nullification of the integral (27) due to the lack of a complete set of Grassmann variables in each term of the integrand.

Below we apply the scheme, described in [20] to obtain the eigenfunctions of the transfer-matrix Hamiltonian (18) in the $m \neq 0$ case. We compute modified expressions for all three subfamilies of radial eigenfunctions. Again, it is possible to get explicit formulae only in large- and small- θ asymptotics and on certain submanifolds even with a massive exploitation of a computer algebra system. These submanifolds are ‘‘bosonic line’’ $\theta_{B2} = \theta_F = 0$ (only θ_{B1} is left) and ‘‘fermionic’’ line $\theta_{B1} = \theta_{B2} = 0$ (only θ_F is left).

Based on the previous works [29, 32, 35] one would expect that the presence of the WZW potential (20) in the $m \neq 0$ case will lead to the emergence of additional eigenfunctions. These eigenfunctions decay exponentially as a function of one or both noncompact angles θ_{B1} , θ_{B2} and thus can be dubbed as (partially) *bound states*. For example, in the symmetry class A the presence of bound states of transfer-matrix Hamiltonian can be demonstrated by applying the Sutherland transform [35]. In class D with one replica this problem was solved in the Ref. 29, where a complete set of bound states was obtained via Iwasawa trick. Moreover, there it was shown that one can incorporate bound states into the heat kernel (13) by a simple shift of the integration contour (sum over μ is interpreted as integral over continuous momentum q in that case).

In general, bound states appear as a satellite set for the main set of propagating eigenfunctions and can be obtained by taking them at certain imaginary values of Iwasawa momenta. In our case, we have two subclasses of unbound eigenfunctions (one- and three-parametric) and we thus expect that both will give rise to bound states in the presence of the WZW term. We claim that all of them can be identified by a careful inspection of the Harish-Chandra c -function, which describes the leading asymptotics of the wavefunctions at large θ . Below we describe in detail this procedure for class D with two replicas and show that the bound states have a rich structure in this case.

We now proceed to the demonstration of results of

the Iwasawa-trick computation of the three- and one-parametric eigenfunctions (according to the scheme outlined in Ref. 20) and then discuss the bound states in detail.

A. Zero mode

It can be checked by a direct computation that the following function is the zero mode of the Hamiltonian (18):

$$\Psi_0 = \left[\frac{\cos^2(\theta/2)}{\cosh(\theta_1/2) \cosh(\theta_2/2)} \right]^m. \quad (28)$$

In the $m = 0$ case this expression equals unity, which is known to be the zero mode in the supersymmetric theories without WZW term.

It is remarkable that in the Iwasawa trick construction, Ψ_0 appears to be a common factor for all the eigenfunctions (27). In particular, it means that wavefunctions automatically nullify at the ‘‘south pole’’ $\theta = \pi$, the property discussed in detail in Ref. [10].

B. Three-parametric subfamily

Three-parametric subfamily is parametrised by two real momenta q_1 and q_2 and by a discrete momentum $l = m, m + 1, \dots$ (see Sec. IID). The relation to the initial Iwasawa momenta [see Eq. (23)] is the following: $p_{B1} = q_1$, $p_{B2} = q_2 - i/2$. Domain $q_1 > q_2 > 0$ covers once all the eigenfunctions of this subclass. Corresponding eigenvalues appear to be m -invariant:

$$\epsilon_{q_1 q_2 l} = \frac{1}{4} + q_1^2 + q_2^2 + \frac{1}{2}l(l+1) \quad (29)$$

As in the $m = 0$ case, three-parametric subfamily vanishes on the bosonic line ($\theta_{B2} = \theta_F = 0$, θ_{B1} left). On the fermionic line ($\theta_{B1} = \theta_{B2} = 0$, θ_F left), we obtained the following expression:

$$\begin{aligned} & \frac{\phi_{q_1 q_2 l}(0, 0, \theta_F)}{\Psi_0} \\ &= 16(l^2 + 4q_1^2)(l^2 + 4q_2^2)P_{l-m}^{(0,2m)}(\lambda_F) \sin^4 \frac{\theta_F}{2} \\ &+ 32 \frac{(1+l+m)(1+l-m)}{1+l} \epsilon_{q_1 q_2 l} \\ &\times \left[P_{l-m}^{(0,2m)}(\lambda_F) - P_{1+l-m}^{(0,2m)}(\lambda_F) \right] \sin^2 \frac{\theta_F}{2}, \quad (30) \end{aligned}$$

where $\lambda_F = \cos \theta_F$ and $P_\nu^{(\alpha,\beta)}$ is the Jacobi function. New features in this expression, compared to the $m = 0$ case are: (i) appearance of Jacobi functions, which are reduced to Legendre functions in the $m = 0$ case, (ii) the fermionic quantum number l takes integer values $l \geq m$ starting from m rather than 0, which is justified by the condition of a proper behaviour of the eigenfunctions at

the origin $\theta_{B1} = \theta_{B2} = \theta_F = 0$, (iii) the wavefunctions gain an overall factor given by the zero mode (28), (iv) algebraic coefficients before the Jacobi functions gain m -dependence.

In the last paragraph of Sec. IID we explained that it is sufficient to consider the values of the wavefunctions only in the Weyl chamber $\theta_{B1} > \theta_{B2} > 0$. Correspondingly, we will consider the asymptotic behaviour at $\theta_{B1}, \theta_{B2} \gg 1$ with $\theta_{B1} > \theta_{B2}$. Then we obtain:

$$\phi_{q_1 q_2 l} \sim \mathcal{W} \tilde{c}_{q_1 q_2 l} \cdot P_{l-m}^{(0,2m)}(\lambda_F) e^{i q_1 \theta_{B1} + (i q_2 + 1/2) \theta_{B2}}, \quad (31)$$

with

$$\tilde{c}_{q_1 q_2 l} \propto \frac{(1+l-2iq_1)(l+2iq_1)(1+l-2iq_2)(l+2iq_2)}{C_{q_1}^m C_{q_2}^m C_{q_1+q_2}^0 C_{q_1-q_2}^0}, \quad (32)$$

where

$$C_{q_1}^m = \frac{\Gamma(1/2 + iq_1 + m/2) \Gamma(1/2 + iq_1 - m/2)}{\Gamma(2iq_1)}. \quad (33)$$

The operator \mathcal{W} denotes isotropization with respect to the Weyl group:

$$\mathcal{W} F_{q_1, q_2} = \sum_{\sigma_1, \sigma_2 = \pm 1} (F_{\sigma_1 q_1, \sigma_2 q_2} + F_{\sigma_1 q_2, \sigma_2 q_1}), \quad (34)$$

where the sum is taken over all possible sign choices [four for each term in (34)].

C. One-parametric subfamily

In Sec. IID we argued that Iwasawa trick requires a modification to get all the eigenfunctions. In Ref. 20 we demonstrated that one can obtain extra class of eigenfunctions by considering (27) at $p_2 = p_3 = 0$, $p_1 = q_1 \neq 0$ in a modified parametrization of the U -integral over K group, which allows to drop redundant integration over some of the Grassman variables. In this case $q_1 > 0$ covers all the eigenfunctions of this subfamily [see the explanation in the end of Sec. IID].

Contrary to three-parametric eigenvalues (29), eigenvalues for the one-parametric subfamily do acquire an m -dependence:

$$\epsilon_{q_1} = q_1^2 + \frac{m^2}{4}. \quad (35)$$

Expression on the fermionic line reads:

$$\frac{\phi_{q_1}(0, 0, \theta_F)}{\Psi_0} = -4\epsilon_{q_1} \sin^2 \frac{\theta_F}{2}, \quad (36)$$

while on the bosonic line the eigenfunctions equal:

$$\frac{\phi_{q_1}(\theta_{B1}, 0, 0)}{\Psi_0} = \frac{i\epsilon_{q_1}}{q_1} \left[P_{iq_1 + \frac{m}{2}}^{(0,-m)}(\lambda_1) - P_{-iq_1 - \frac{m}{2}}^{(0,-m)}(\lambda_1) \right], \quad (37)$$

where $\lambda_1 = \cosh \theta_{B1}$. As in the $m = 0$ case [20], this expression completely coincides with the transfer-matrix Hamiltonian eigenfunctions of the one-replica sigma model [29]. Thus, one-parametric subclass of eigenfunctions $\phi_{q_1}(\theta_{B1}, \theta_{B2}, \theta_F)$ can be viewed as an extension of one-replica expression $\phi_{q_1}(\theta_{B1}, 0, 0) = \phi_{q_1}(\theta_{B1})$ to a higher-dimensional manifold.

D. Bound states from the one-parametric subfamily

As explained above, WZW term leads to the emergence of the additional bound states of the Hamiltonian (18). A part of them can be readily identified by considering the heat kernel (13) at the bosonic line $\theta_{B2} = \theta_F = 0$. As the Jacobian (10) and potential (20) on this line reduce to their one-replica values, we must reproduce one-replica heat kernel at this line. Indeed, according to Sec. III B and Sec. III C three-parametric wavefunctions vanish at this line while the one-parametric eigenfunctions coincide with the one-replica eigenfunctions. But from Ref. 29 we know that at $m \neq 0$ one-replica eigenbasis contains also a set of bound states, obtainable from the main set of eigenfunctions $\phi_{q_1}(\theta)$ by taking certain imaginary values of momentum q_1 , which we list in the second column of Table II for $m = 1, \dots, 7$. Thus, to make the heat kernel complete at the bosonic line, we must add to the basis one-parametric eigenfunctions $\phi_{q_1}(\theta_{B1}, \theta_{B2}, \theta_F)$ taken at that values of q_1 :

$$\tilde{\phi}^{(j)} = \phi_{q_1 = s_j}, \quad s_j \in \mathcal{S}^{1P}, \quad (38)$$

where \mathcal{S}^{1P} is presented in Table II.

E. Bound states from three-parametric subfamily and general algorithm

In Sec. III D we described the bound states, generated by the one-parametric subfamily of eigenfunctions. Now we study the bound states, related to the three-parametric subfamily and describe the general algorithm for this procedure.

To start, let us rewrite the θ_{B1}, θ_{B2} -dependent part of the asymptotics (31) in a more explicit form. In order to study whether a function can be normalised we also multiply it by the square root of the Jacobian (10) and get:

$$\sqrt{J} \phi_{q_1 q_2 l} \sim \sum_{w=1}^8 \tilde{c}_{q_1^{(w)} q_2^{(w)} l} e^{i q_1^{(w)} \theta_{B1} + i q_2^{(w)} \theta_{B2}}, \quad (39)$$

where $q_1^{(w)}$ and $q_2^{(w)}$ take values listed in Table III. Equation (39) is an explicit form of the symmetrisation (34).

To check that the wavefunction (39) is normalisable in the Weyl chamber $\theta_{B1} > \theta_{B2} > 1$, it suffices to try its values at the boundaries, which are formed by two rays:

TABLE II. Values of imaginary momenta, corresponding to the (partially) bound states with the respect to the non-compact variables θ_{B1} , θ_{B2} . \mathbf{S}^{1P} corresponds to the bound states, related to the one-parametric subfamily, while \mathbf{S}^{3P} and $\mathbf{S}^{3P'}$ correspond to the bound state, generated by the three-parametric eigenfunctions. See Sec. III D and III E for the explanation.

m	\mathbf{S}^{1P}	j	\mathbf{S}^{3P}	$\mathbf{S}_j^{3P'}$
0				
1				
2		1	$i/2$	
3	$i/2$	1	i	$i/2$
4	i	1	$i/2$	
		2	$3i/2$	i
5	$i/2, 3i/2$	1	i	$i/2$
		2	$2i$	$i/2, 3i/2$
6	$i, 2i$	1	$i/2$	
		2	$3i/2$	i
		3	$5i/2$	$i, 2i$
7	$i/2, 3i/2, 5i/2$	1	i	$i/2$
		2	$2i$	$i/2, 3i/2$
		3	$3i$	$i/2, 3i/2, 5i/2$

$\theta_{B2} = 0$, $\theta_{B1} > 0$ and $\theta_{B1} = \theta_{B2} > 0$. This way one can easily formulate the condition for the function (39) to be normalizable:

For each term that has $\text{Im } q_1^{(w)} < 0$ or $\text{Im } q_1^{(w)} + q_2^{(w)} < 0$ (and which is thus non-normalizable) the corresponding coefficient should nullify: $\tilde{c}_{q_1^{(w)}, q_2^{(w)}}^{(w)l} = 0$.

To apply this algorithm for the identification of the bound states one can search among the zeros of the Harish-Chandra c -function (32) and then check for the above condition to hold. Following this procedure we identified the following bound states:

$$\tilde{\phi}_{q_2, l}^{(j)} = \phi_{s_j, q_2, l}, \quad s_j \in \mathbf{S}^{3P}, \quad q_2 \in \mathbb{R}; \quad (40a)$$

$$\tilde{\phi}_l^{(j, k)} = \phi_{s_j, t_k, l}, \quad s_j \in \mathbf{S}^{3P}, \quad t_k \in \mathbf{S}_j^{3P'}. \quad (40b)$$

The first subclass is formed by fixing q_1 at a certain imaginary value, while q_2 is an arbitrary real number. The second subclass is formed by fixing both q_1 and q_2 at some imaginary values. These values are presented in Table II. Discrete parameter l takes any integer value in the range $l \geq m$.

Note that Eqs. (40) represent all bound states and one should not add expressions obtained by substitutions $q_{1,2} \rightarrow -q_{1,2}$ or $q_1 \leftrightarrow q_2$. The reason is that three-parametric wavefunctions $\phi_{q_1 q_2 l}$ are fully symmetric with respect to the Weyl group acting on q_1 and q_2 . That's why mentioned substitutions will not produce any new eigenfunctions.

We obtained that for the main three-parametric subfamily of eigenfunctions there exist two subclasses of bound states, obtained by fixing one/two of the mo-

TABLE III. List of substitutions forming the Weyl group in the boson-boson sector of the theory, see Eqs. (34) and (39).

w	1	2	3	4	5	6	7	8
$q_1^{(w)}$	q_1	$-q_1$	q_1	$-q_1$	q_2	$-q_2$	q_2	$-q_2$
$q_2^{(w)}$	q_2	q_2	$-q_2$	$-q_2$	q_1	q_1	$-q_1$	$-q_1$

menta q_1, q_2 at certain imaginary values. We propose that this phenomenon can be generalised to all subfamilies of eigenfunctions in the sigma-models with an arbitrary number of replicas. For an eigenfunction subfamily, dependent on a set of momenta q_1, \dots, q_s one would found bound states, obtained by fixing any subset of q_1, \dots, q_s at certain imaginary values (for sufficiently large m). These bound states for all higher-rank sigma-models can be identified by a direct generalisation of the presented criterion. The sum in the analog of (39) is to be performed over the Weyl group substitutions, acting on q_1, \dots, q_s .

IV. HEAT KERNEL CONSTRUCTION

The heat kernel is constructed from the eigenfunctions of the Hamiltonian according to Eq. (13), where all classes of eigenfunctions contribute. Integrals and sums over Iwasawa momenta are to be performed with some measure, denoted by μ_ν in Eq. (13). For noncompact spaces, Plancherel determined that this measure can be expressed via the coefficient before the large- θ asymptotics (Harish-Chandra c -function): $\mu_\nu = 1/|c_\nu|^2$ [33]. Later, it became a common knowledge that a straightforward generalisation provides a correct measure for the supersymmetric case [27, 32]. Here and in Ref. 29 we make a further step and claim that expression for the Plancherel measure works even in the presence of the vector potential in the Hamiltonian (14) generated by the WZW term.

To evaluate the coefficient c_ν for the bound states, one should take the contribution of the propagating wavefunctions of the same subfamily (one- or three-parametric) and take residues in the poles at imaginary Iwasawa momenta corresponding to each bound state. We check that our construction of the heat kernel works on the fermionic line $\theta_{B1} = \theta_{B2} = 0$ following the scheme outlined in Appendix E of Ref. [20]. Also, a good verification is provided by the fact that we obtained sensible results for the transport properties of the wire at small L from the constructed heat kernel. Namely, for conductance variance, we observed cancellation of L^{-2} and L^{-1} terms in the small- L expansion, leading to a finite value in the Ohmic regime as predicted by the theory of universal conductance fluctuations [36].

The measure for the three-parametric subfamily can be evaluated according to the formula from the Ref. [20] (but

l now takes values starting from m : $l = m, m + 1, \dots$):

$$\mu_{q_1 q_2 l} = \text{res}_l \frac{1}{c_{q_1 q_2 l} c_{-q_1, -q_2, -1-l}}, \quad (41)$$

where $c_{q_1 q_2 l} = \tilde{c}_{q_1 q_2 l} / (\pi c_{-i(l+1/2)})$ and $c_q = iqC_q$.

Analogously, for the one-parametric subfamily the measure is given by:

$$\mu_{q_1} = \frac{1}{2\pi} \frac{1}{c_{q_1} c_{-q_1}}. \quad (42)$$

We now present the final expression for the heat kernel (13) as a sum over all the subfamilies and subclasses of the Laplacian eigenbasis:

$$\psi(Q, L) = \Psi_0 + \Psi_1 + \Psi_1^{\text{res}} + \Psi_3 + \Psi_3^{\text{res}} + \Psi_3^{\text{d.res}}. \quad (43)$$

It contains the following contributions:

- The zero mode (28), which is the common factor for all the eigenfunctions according to Eq. (27).
- One-parametric subfamily, inherited from the one-replica sigma-model:

$$\Psi_1 = 2 \int_0^\infty dq \mu_q \phi_q. \quad (44)$$

- Bound states for the one-parametric subfamily (38):

$$\Psi_1^{\text{res}} = -2\pi i \sum_{s_j \in \mathcal{S}^{1P}} \text{res}_{q=s_j} \mu_q \phi_q. \quad (45)$$

As the previous contribution, it is inherited from the $n = 1$ case. The sets of discrete imaginary momenta \mathcal{S}^{1P} are listed in Table II for $m = 0 \dots 7$.

- Three-parametric contribution regularly obtained via the Iwasawa trick:

$$\Psi_3 = 4 \int_0^\infty dq_2 \int_0^{q_1} dq_1 \sum_{l=m}^\infty \mu_{q_1 q_2 l} \phi_{q_1 q_2 l}. \quad (46)$$

- Bound states (in one direction) for three-parametric contribution (40a):

$$\Psi_3^{\text{res}} = -8\pi i \int_0^\infty dq_2 \sum_{s_j \in \mathcal{S}^{3P}} \text{res}_{q_1=s_j} \sum_{l=m}^\infty \mu_{q_1 q_2 l} \phi_{q_1 q_2 l}. \quad (47)$$

The points \mathcal{S}^{3P} are listed in Table II for $m = 0 \dots 7$.

- Bound states (in both θ_{B1} and θ_{B2}) for three-parametric contribution (40b):

$$\Psi_3^{\text{d.res}} = -8\pi^2 \sum_{s_j \in \mathcal{S}^{3P}} \sum_{t_k \in \mathcal{S}_j^{3P'}} \text{res}_{q_2=t_k} \text{res}_{q_1=s_j} \sum_{l=m}^\infty \mu_{q_1 q_2 l} \phi_{q_1 q_2 l}. \quad (48)$$

The points $\mathcal{S}_j^{3P'}$ are listed in Table II.

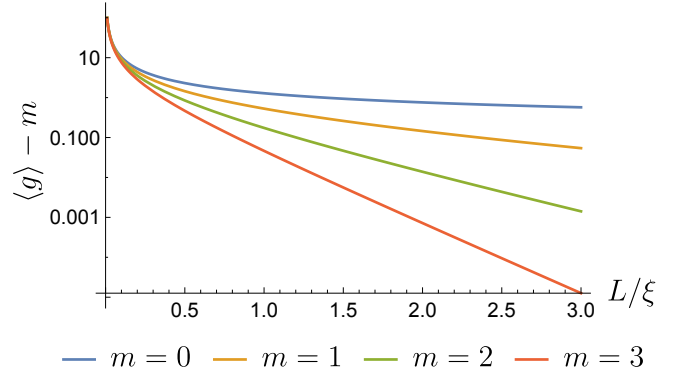


FIG. 3. Contribution of unprotected modes to the disorder-averaged conductance in the presence of m protected topological modes as a function of the wire length L , logarithmic scale.

Equations (43)–(48) define six contributions to the heat kernel (43). Each term is an integral/sum over eigenfunctions, where each eigenfunction is counted only once. However, sometimes it is convenient to extend by symmetry the integrals over q_1 and q_2 to the full axis $(-\infty, +\infty)$ and correspondingly adjust the number before the integral. This representation allows to shift the contour of integration in the complex plane. It is known that in a one-replica sigma-model one can shift the contour of integration across the poles in the integrand in a way that corresponding residues will completely cancel contribution of the bound states [29]. Then, the heat kernel can be represented without extra terms compared to the $m = 0$ case. As explained above, one-parametric subfamily of eigenfunctions is directly related to the one-replica eigenfunctions, so we can follow Ref. 29 and replace the integral in (44) to an integral along the contour $(-\infty + i[m-1+0], +\infty + i[m-1+0])$ without a factor 2 before the integral. That will not change the heat kernel (43) provided we exclude the bound-state contribution (45).

It seems tempting to find an analogous contour shift for the regular three-parametric contribution (46) to get rid of subsidiary contributions (47) and (48). We did not find a corresponding shift that would eliminate both (47) and (48), but we found that one can get rid of (48). To do this, in the expression (47) one should integrate over the variable $q_+ = q_1 + q_2$ along the contour $(-\infty, +\infty)$ with an overall coefficient $-4\pi i$ instead of $-8\pi i$.

V. RESULTS

Transport characteristics of the system can be evaluated from Eq. (9) with the partition function (11) provided by the constructed heat kernel (43). Expression (9) implies taking partial derivatives along the directions corresponding to different θ_i . We cannot calculate the mixed derivatives directly, as we did not obtain

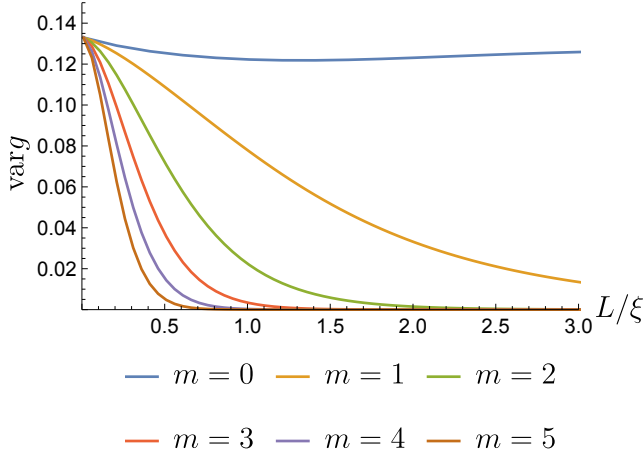


FIG. 4. Variance of quasiparticle conductance in the presence of m protected topological modes as a function of the wire length L .

the wavefunctions on the whole manifold in an explicit form. However, in Ref. 20 we argued that it is sufficient to know θ_F -derivatives only, because the rest can be expressed by applying the Schrodinger equation (12) to the small- θ expansion. That means that we can calculate transport characteristics from the values of the heat kernel on the ‘fermionic’ line provided by substitution of Eqs. (30) and (36) into (43). Note that only the zero mode and one-parametric eigenfunctions [along with the related bound states (45)] contribute to the average conductance as the expansion of the other terms is quartic at small θ_i . The calculation includes complicated integrations/summations over Iwasawa momenta in Eqs. (44)–(48), which allows to obtain analytical expressions only in the asymptotical regimes. We provide the corresponding results below and then discuss the behaviour at arbitrary L presented graphically in Fig. 2–6. We demonstrate results for the $m = 0$ case but do not discuss them in detail as it was done in Ref. 20.

In the long-wire limit, $L \gg \xi$, the asymptotic behaviour of conductance moments is determined by eigenfunctions with the lowest eigenvalue ϵ_ν , since they contribute the slowest exponential to the heat kernel (13). The case with $m = 0$ was discussed in detail in Ref. 20. For $m = 1$ and $m = 2$ cases, these eigenfunctions are the ones from the one-parametric subfamily (44) with $q_1 \sim 0$. We then use the steepest decent method to obtain the asymptotics. Starting from $m = 3$, the lowest eigenvalue corresponds to the bound state, which originates from the one-parametric subfamily by taking the largest imaginary momentum $s_j = i(m - 2)/2$ from the allowed set [see \mathcal{S}^{1P} column of Table II and Eq. (45)]. That bound state has the lowest exponent, since imaginary momentum contributes negatively to the eigenvalue: $\epsilon_{s_j} = m^2/4 - |s_j|^2$. Within described approach, we obtain

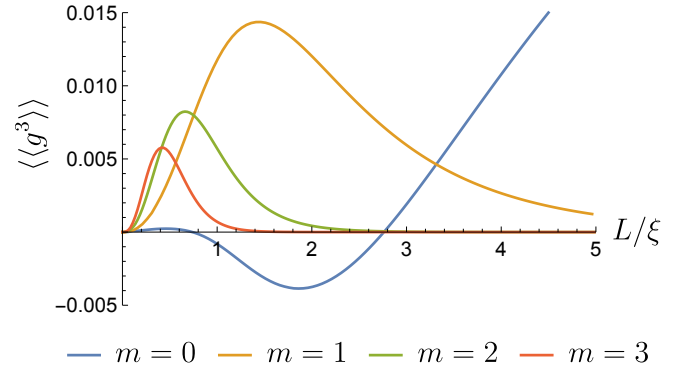


FIG. 5. Third cumulant $\langle\langle g^3 \rangle\rangle$ of quasiparticle conductance in the presence of m protected topological modes as a function of the wire length L .

the following asymptotics for conductance moments:

$$\langle g^l \rangle - m^l \sim \alpha_i^{(m)} \begin{cases} g_L, & m = 0, \\ g_L(\xi/L)e^{-L/2\xi}, & m = 1, \\ g_L e^{-2L/\xi}, & m = 2, \\ e^{-2(m-1)L/\xi}, & m \geq 3, \end{cases} \quad (49)$$

where $g_L = \sqrt{2\xi/\pi L}$ and numerical coefficients $\alpha_i^{(m)}$ are given in Table IV for different m . Similar expressions work also for the Fano factor, so we give the corresponding numbers in the last line of the same table.

The short-wire limit, $L \ll \xi$, is most easily accessed via direct perturbative solution of the Schrödinger equation for the heat kernel [32]. The corresponding calculation is a straightforward generalisation of the calculation in the absence of the WZW term that can be found in Ref. [20]. The resulting expansions for $\langle g \rangle$, $\text{var } g = \langle g^2 \rangle - \langle g \rangle^2$, $\langle\langle g^3 \rangle\rangle = \langle g^3 \rangle - 3\langle g^2 \rangle \langle g \rangle + 2\langle g \rangle^3$, and the Fano factor F read:

$$\langle g \rangle = \frac{\xi}{L} + \frac{1}{3} + \left(\frac{m^2}{3} - \frac{1}{15} \right) \frac{L}{\xi} + \left(\frac{2}{63} - \frac{2m^2}{15} \right) \frac{L^2}{\xi^2} + \dots, \quad (50a)$$

$$\text{var } g = \frac{2}{15} - \frac{8}{315} \frac{L}{\xi} + \left(\frac{136}{4725} - \frac{34m^2}{315} \right) \frac{L^2}{\xi^2} + \dots, \quad (50b)$$

$$\langle\langle g^3 \rangle\rangle = \frac{8}{1485} \frac{L^2}{\xi^2} + \left(\frac{11056m^2}{155925} - \frac{120704}{6449625} \right) \frac{L^3}{\xi^3} + \dots \quad (50c)$$

$$F = \frac{1}{3} - \frac{4}{45} \frac{L}{\xi} + \left(\frac{76}{945} - \frac{4m^2}{15} \right) \frac{L^2}{\xi^2} + \dots \quad (50d)$$

In the process of $\text{var } g$ calculation, two leading terms proportional to $1/L^2$ and $1/L$ completely cancel, as expected for universal conductance fluctuations [36].

At arbitrary L , integrations and summations over Iwasawa momenta in Eqs. (44)–(48) should be performed

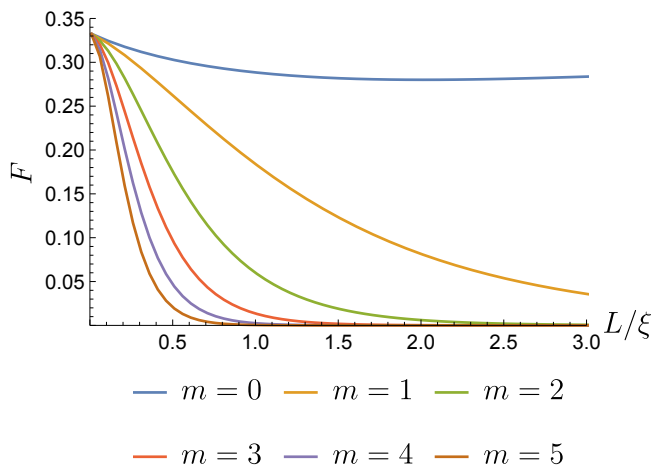


FIG. 6. Pseudo-Fano factor in the presence of m protected topological modes as a function of the wire length L .

numerically. The result for the disorder-averaged conductance is presented in Fig. 2 (it can be also found in the Thesis [29]). In this graph one can clearly see the crossover from the Drude regime at $L \ll \xi$ to the peculiar regime at large lengths. The first one demonstrates the behaviour, typical for a diffusive metal, where conductance scales as $\langle g \rangle \sim \xi/L$ and no signatures of topological modes are visible. At very large lengths, only contribution of the topologically protected modes survives, as expected. Extra contribution of unprotected modes decays exponentially according to the localization scenario. To compare the exponents of this process at different m , we plot $\langle g \rangle - m$ in the logarithmical scale in Fig. 3 [see also Eq. (49)]. Note that the localization length for non-topological modes decreases with increasing the number of topological modes m , leading to a quicker decay of conductance. Finally, at $m = 0$ the conductivity decays much slower according to a power law $\langle g \rangle \sim \sqrt{\xi/L}$, since it describes a critical Majorana wire as described in detail in Ref. 20.

Results for the conductance variance for a broad range of system length L can be found in Fig. 4. In the Ohmic regime at small L the variance takes a universal m -independent value of $2/15$. This observation is explained by the theory of universal conductance fluctuations [36]. At large L the variance drops exponentially for $m \neq 0$ since non-topological modes are suppressed and contribution of topological modes does not fluctuate from sample to sample.

In Fig. 5 we present our result for the third cumulant of the conductance $\langle\langle g^3 \rangle\rangle = \langle g^3 \rangle - 3\langle g^2 \rangle \langle g \rangle + 2\langle g \rangle^3$. The curve for the $m = 0$ case eventually decays $\sim L^{-1/2}$ at very large lengths $L \gtrsim 30$ as was shown in Ref. 20. For $m \neq 0$ the decay is exponential as expected. Remarkably, for any m , $\langle\langle g^3 \rangle\rangle$ behaves as L^2 at small length because the linear term vanishes unexpectedly. However, similar cancellation of the leading contribution was reported

TABLE IV. Numerical factor $\alpha_i^{(m)}$ in the large- L asymptotics (49) of conductance moments $\langle g^i \rangle$ and pseudo-Fano factor.

	$m = 0$	$m = 1$	$m = 2$	$m \geq 3$
$\langle g \rangle$	1	$\pi^2/4$	1	$m - 2$
$\langle g^2 \rangle$	$2/3$	$13\pi^2/24$	4	$2m(m - 2)$
$\langle g^3 \rangle$	$8/15$	$143\pi^2/160$	12	$3m^2(m - 2)$
F	$1/(3g_L)^a$	$\pi^2/8$	$2/3$	$2(m - 2)/3$

^a In the $m = 0$ case pseudo-Fano factor does not decay like conductance moments ($\propto g_L$), but approaches asymptotical value $1/3$ due to the Dorokhov distribution of the critical channel transparency [20].

in the weak-localization regime for the one-dimensional geometry in Ref. 37.

Pseudo-Fano factor for various lengths can be found in Fig. 6, which is similar to the graph for the variance. Again, in the short-length limit one observes m -independent finite value $1/3$. This value was predicted for a diffusive metal, described by Dorokhov bimodal distribution of transmission eigenvalues [38]. At large length all the curves ($m \neq 0$) decay exponentially for the same reason as for the variance: non-topological modes localize and topological contribution is quantized and thus does not have a shot noise.

VI. CONCLUSION

In the present paper we performed an extensive study of superconducting quasi-1D systems of symmetry class D with topologically protected modes. Such systems can arise at the boundary of 2D topological superconductors with broken time-reversal and spin-rotational systems. In the text, we suggested a particular way of constructing a system with both topological and regular modes by making an interface between two 2D samples with different values of \mathbb{Z} -topological index (Fig. 1). However, our results are not restricted by this particular geometry and can be applied to any 1D system, provided the number of conducting channels is large.

For wires of arbitrary length, we report on exact expressions for the average thermal conductance, its variance, and third cumulant, as well as the shot noise power. The average conductance was evaluated previously in Ref. [29], where a minimal one-replica version of the sigma-model was used. In our work we resorted to the two-replica nonlinear supersymmetric sigma-model, which allows to access higher moments of transport characteristics.

As was argued in Ref. [20], in principle, one can extract the full counting statistics (FCS) from the two-replica sigma model in class D. Indeed, distribution of transmission probabilities is expressed via the heat kernel in the vicinity of the ‘‘supersymmetric line’’ $\theta_{B1} = \theta_{B2} = -i\theta_F$. There is no such line in one-replica model due to the de-

generacy of the compact sector of the theory. However we did not present explicit results for FCS due to a very complicated structure of the integral representation (27) in the Iwasawa trick construction, which prevents righting the heat kernel in the analytical form on the supersymmetric line. Instead, we evaluated the heat kernel at other submanifolds, which suffices to calculate a number of physical quantities mentioned above.

Our findings illustrate in detail the crossover from the Ohmic regime at small lengths to the regime of developed localization at large lengths. In particular, we showed that the presence of topologically protected modes enhances localization of unprotected modes. Results for the average conductance $\langle g \rangle$ coincide with the results obtained from a simpler (one-replica) sigma-model in Ref. 29. However, as we obtain them from a more complicated two-replica theory, such a coherence is an extra check for our construction.

As we study a superconducting class without a spin-rotational symmetry, experimental verification of our results requires thermal transport measurements. That could be a challenging task, however, recent developments indicate that such measurements are possible at a mesoscopic scale [39, 40]. To perform disorder-averaging experimentally, one can use a common trick of varying magnetic field or chemical potential in a range that preserves topological state in the system but effectively perturbs the disorder potential.

From a technical perspective, calculation of the heat kernel boils down to finding the radial eigenbasis of the transfer-matrix Hamiltonian. In our previous work [20] we considered class D sigma-model without protected modes, where the Hamiltonian was given by the Laplace-Beltrami operator on the sigma-model supermanifold. Here, topological modes described by a WZW term in the sigma-model action introduce a vector potential to the Laplacian. For a one-replica case, this vector potential has a special form and does not affect the milestones of the Iwasawa trick solution for the heat kernel [29]. However, the existing eigenfunctions are modified by the WZW term and additional bound states arise in the eigenbasis. In our work we confirmed that Iwasawa trick works in the two-replica theory of class D as well. In particular, our results confirm that the Plancherel measure provides a valid expression even in the presence of the WZW term. However, in the two-replica theory, emerging bound states have a much richer structure. Even in the absence of the WZW term, there were two subfamilies of eigenfunctions and a zero mode in the eigenbasis [20]. We showed that both subfamilies give rise to a number of bound states. Moreover, the three-parametric subfamily produces two subclasses of bound states that are localized in one/two directions in the noncompact sector.

We presented a scheme that allows to identify the bound states algorithmically. This algorithm can be straightforwardly extended to class D sigma-model with three and more replicas as well as to the sigma-models of other symmetry classes. In particular, the scheme can

explain the bound states that were found in Ref. 32 for the symplectic symmetry class. That comprises a development in the radial Fourier analysis on the symmetric superspaces and can be used in physical applications.

ACKNOWLEDGMENTS

This work was partially supported by the Russian Science Foundation under Grant No. 20-12-00361.

Appendix A: Evaluation of the gauge factor $\text{sdet } K_I$

In this Appendix, we present the algebra that allows to express the gauged wavefunction (26) as the function of Cartan variables θ_i and U [Eq. (27)]. To starting point is to find the gauge factor V by equating Eqs. (17) and (21) taking into account the gauge change (25):

$$T = U^{-1} e^{\tilde{\theta}/2} U = V e^{\tilde{a}/2} N. \quad (\text{A1})$$

Remember that U and V matrices belong to the K group of Λ -commuting matrices, $\tilde{\theta}$ and \tilde{a} are Cartan and Iwasawa radial angles, correspondingly. Matrix N appears in the Iwasawa decomposition (21) and is an upper-triangular matrix with units on the main diagonal.

Matrices, used in Eq. (A1) have the following block structure:

$$\tilde{\theta} = \begin{pmatrix} \tilde{\theta} & 0 \\ 0 & -R\tilde{\theta}R \end{pmatrix}, \quad \tilde{a} = \begin{pmatrix} \tilde{a} & 0 \\ 0 & -R\tilde{a}R \end{pmatrix}, \quad (\text{A2a})$$

$$\Lambda = \begin{pmatrix} 0 & R \\ R & 0 \end{pmatrix}, \quad e^{\tilde{a}/2} N = \begin{pmatrix} X & Y \\ 0 & Z \end{pmatrix}, \quad (\text{A2b})$$

where R is a 4×4 matrix with unities at the anti-diagonal, $\tilde{\theta} = \text{diag} \{ \theta_{B1}, \theta_{B2}, i\theta_F, i\theta_F \}$ and $\tilde{a} = \text{diag} \{ a_{B1}, a_{B2}, ia_F, ia_F \}$. The blocks X , Y and Z contain Iwasawa coordinates and constitute an upper triangular matrix $e^{\tilde{a}/2} N$. So, the blocks X and Z are themselves upper triangular and contain exponentials of Iwasawa angles $e^{a_i/2}$ on the main diagonal.

To allow further calculations, we find it useful to consider a basis rotation, in which all matrices appear as blocks arranged in Nambu space. In symmetry class D, Nambu space plays the role of the retarded-advanced (RA) space, so in the following we will term the blocks using the RA-terminology. We denote the desired rotation by matrix L and emphasize that it brings Λ to the diagonal form:

$$L = \frac{1}{\sqrt{2}} \begin{pmatrix} \mathbf{1} & \mathbf{1} \\ R & -R \end{pmatrix}, \quad L^T \Lambda L = \begin{pmatrix} \mathbf{1} & 0 \\ 0 & -\mathbf{1} \end{pmatrix}. \quad (\text{A3})$$

The other objects transform in the following way:

$$L^T U L = \begin{pmatrix} U_R & 0 \\ 0 & U_A \end{pmatrix}, \quad L^T e^{\frac{\tilde{\theta}}{2}} L = \begin{pmatrix} \cosh \frac{\tilde{\theta}}{2} & \sinh \frac{\tilde{\theta}}{2} \\ \sinh \frac{\tilde{\theta}}{2} & \cosh \frac{\tilde{\theta}}{2} \end{pmatrix}, \quad (\text{A4a})$$

$$L^T V L = \begin{pmatrix} V_R & 0 \\ 0 & V_A \end{pmatrix}, \quad L^T Q L = \begin{pmatrix} Q_{RR} & Q_{RA} \\ Q_{AR} & Q_{AA} \end{pmatrix}. \quad (\text{A4b})$$

Note that U and V matrices commute with Λ and thus are block-diagonal in the new basis. The first column illustrates this property and gives definition for $U_{R(A)}$ and $V_{R(A)}$ (actually only one of the retarded/advanced blocks of U and V matrices is independent as the other one can be obtained by the charge conjugation operation). That definition allows to express the gauge factor in Eq. (26) in the following way:

$$e^{-\frac{m}{2} \text{str } \Lambda V} = \text{sdet}^{-m/2} V_R \text{sdet}^{m/2} V_A = \text{sdet}^m V_R, \quad (\text{A5})$$

where we assumed that the group element V has unitary determinant.

Now we apply L -rotation to the identity (A1), single out the upper-left (RR) block and evaluate its superdeterminant ($\text{sdet}[L^T T L]_{RR}$) to get:

$$\text{sdet} \cosh \frac{\tilde{\theta}}{2} = \text{sdet} V_R \text{sdet}(X + YR + RZR). \quad (\text{A6})$$

We then single out from this expression $\text{sdet} RZR = \text{sdet} e^{-\tilde{a}/2}$ (here we used that RZR is a triangular matrix with $e^{-\tilde{a}/2}$ on the main diagonal):

$$\frac{\text{sdet} \cosh \frac{\tilde{\theta}}{2}}{\text{sdet} V_R} = \text{sdet} e^{-\tilde{a}/2} \text{sdet}(1 + RZ^{-1}RX + RZ^{-1}RYR). \quad (\text{A7})$$

We have thus expressed $\text{sdet} V_R$ in terms of the Iwasawa coordinates contained in X , Y , and Z .

To simplify the expression further, consider the matrix $\Lambda Q = \Lambda N^{-1} \Lambda N$ is the block-matrix notations (A2):

$$\begin{pmatrix} RZ^{-1}RX & RZ^{-1}RY \\ -RX^{-1}YZ^{-1}RX & -RX^{-1}YZ^{-1}RY + RX^{-1}RZ \end{pmatrix}. \quad (\text{A8})$$

The first row of this matrix contains exactly the blocks we need for Eq. (A7). We can then readily write them in terms of the blocks of Q (in the main basis):

$$\begin{aligned} \text{sdet}(1 + RZ^{-1}RX + RZ^{-1}RYR) \\ = \text{sdet} \left[1 + \begin{pmatrix} 1 & 0 \\ 0 & R \end{pmatrix} \Lambda Q \begin{pmatrix} 1 \\ R \end{pmatrix} \right]. \end{aligned} \quad (\text{A9})$$

We now use L -rotated expression for Q matrix (A4b) by substituting $Q = LQ_{RA}L^T$:

$$\begin{aligned} \text{sdet}(1 + RZ^{-1}RX + RZ^{-1}RYR) \\ = \text{sdet}(1 + Q_{RR} - Q_{AR}). \end{aligned} \quad (\text{A10})$$

Then we evaluate the blocks Q_{RR} and Q_{AR} from the definition $Q = U^{-1} \Lambda e^{\tilde{\theta}} U$ using expressions (A4b) obtained after the L -rotation:

$$\begin{aligned} \text{sdet}(1 + Q_{RR} - Q_{AR}) \\ = \text{sdet} \cosh \frac{\tilde{\theta}}{2} \text{sdet} \left(\cosh \frac{\tilde{\theta}}{2} + U_R U_A^{-1} \sinh \frac{\tilde{\theta}}{2} \right). \end{aligned} \quad (\text{A11})$$

Substituting Eq. (A11) into (A6) allows to express $\text{sdet} V_R$ in terms of Cartan variables θ_i and U . However, it appears to be useful to apply an additional transformation that would allow to single out the common factor for all the eigenfunctions.

Consider $\text{sdet} RZ^{-1}RX$. On the one hand, it can be easily expressed via $\text{sdet} X$ and $\text{sdet} Z$, which are triangular matrices with Iwasawa angles on the main diagonal according to the definition (A2). On the other hand, $RZ^{-1}RX$ equals $(\Lambda Q)_{RR}$ block according to Eq. (A8). Analogously to (A11) we get

$$\text{sdet} e^{\tilde{a}} = \text{sdet}(Q_{RR} + Q_{RA} - Q_{AR} - Q_{AA}). \quad (\text{A12})$$

Evaluating blocks of Q matrix similarly to (A11), we obtain after some algebra:

$$\begin{aligned} \text{sdet} \left[\cosh \frac{\tilde{\theta}}{2} + U_R U_A^{-1} \sinh \frac{\tilde{\theta}}{2} \right] \\ = \text{sdet} e^{\tilde{a}} \text{sdet}^{-1} \left[\cosh \frac{\tilde{\theta}}{2} + \sinh \frac{\tilde{\theta}}{2} U_A U_R^{-1} \right]. \end{aligned} \quad (\text{A13})$$

Substituting (A13) in (A11) and then in (A6) we get

$$\text{sdet} V_R = \text{sdet} e^{-\tilde{a}/2} \text{sdet} \left(\cosh \frac{\tilde{\theta}}{2} + \sinh \frac{\tilde{\theta}}{2} U_A U_R^{-1} \right). \quad (\text{A14})$$

This finishes the derivation of the factor $\text{sdet} V$ in (26) in terms of Cartan variables. We substitute (A14) into (26) and single out the factor $\text{sdet}^{-m} \cosh \tilde{\theta}/2$. Remarkably, it appears to be the zero mode of the transfer-matrix Hamiltonian (18):

$$\Psi_0 = \text{sdet}^{-m} \cosh \frac{\tilde{\theta}}{2}. \quad (\text{A15})$$

Its explicit expression in terms of θ_i is provided in (28).

Using (A14) we straightforwardly bring (26) to the form, used in (27). The next step would be to get rid of unwanted U -dependence by an isotropisation procedure [20, 32]. We perform such an isotropization with the help of a computer algebra system.

-
- [1] P. W. Anderson, "Absence of diffusion in certain random lattices," *Phys. Rev.* **109**, 1492 (1958).
- [2] F. Evers and A. D. Mirlin, "Anderson transitions," *Rev. Mod. Phys.* **80**, 1355 (2008).
- [3] S. M. Girvin and R. Prange, "The quantum hall effect," (1987).
- [4] M. Z. Hasan and C. L. Kane, "Colloquium: Topological insulators," *Rev. Mod. Phys.* **82**, 3045 (2010).
- [5] D. A. Abanin, E. Altman, I. Bloch, and M. Serbyn, "Colloquium: Many-body localization, thermalization, and entanglement," *Rev. Mod. Phys.* **91**, 021001 (2019).
- [6] E. Abrahams, P. W. Anderson, D. C. Licciardello, and T. V. Ramakrishnan, "Scaling theory of localization: Absence of quantum diffusion in two dimensions," *Phys. Rev. Lett.* **42**, 673 (1979).
- [7] P. W. Brouwer, A. Furusaki, I. A. Gruzberg, and C. Mudry, "Localization and delocalization in dirty superconducting wires," *Phys. Rev. Lett.* **85**, 1064 (2000).
- [8] A. Altland, D. Bagrets, and A. Kamenev, "Topology versus Anderson localization: Nonperturbative solutions in one dimension," *Phys. Rev. B* **91**, 085429 (2015).
- [9] A. R. Akhmerov, J. P. Dahlhaus, F. Hassler, M. Wimmer, and C. W. J. Beenakker, "Quantized conductance at the Majorana phase transition in a disordered superconducting wire," *Phys. Rev. Lett.* **106**, 057001 (2011).
- [10] E. Khalaf, M. A. Skvortsov, and P. M. Ostrovsky, "Semiclassical electron transport at the edge of a two-dimensional topological insulator: Interplay of protected and unprotected modes," *Phys. Rev. B* **93**, 125405 (2016).
- [11] A. Kitaev, "Periodic table for topological insulators and superconductors," *AIP Conf. Proc.* **1134**, 22 (2009).
- [12] S. Ryu, A. P. Schnyder, A. Furusaki, and A. W. W. Ludwig, "Topological insulators and superconductors: tenfold way and dimensional hierarchy," *New J. Phys.* **12**, 065010 (2010).
- [13] A. Mildenberger, F. Evers, A. D. Mirlin, and J. T. Chalker, "Density of quasiparticle states for a two-dimensional disordered system: Metallic, insulating, and critical behavior in the class-d thermal quantum hall effect," *Phys. Rev. B* **75**, 245321 (2007).
- [14] N. Read and D. Green, "Paired states of fermions in two dimensions with breaking of parity and time-reversal symmetries and the fractional quantum hall effect," *Phys. Rev. B* **61**, 10267 (2000).
- [15] M. Grayson, D. Schuh, M. Huber, M. Bichler, and G. Abstreiter, "Corner overgrowth: Bending a high mobility two-dimensional electron system by 90," *Applied Physics Letters* **86**, 032101 (2005).
- [16] M. Grayson, L. Steinke, D. Schuh, M. Bichler, L. Hoepfel, J. Smet, K. v. Klitzing, D. K. Maude, and G. Abstreiter, "Metallic and insulating states at a bent quantum hall junction," *Phys. Rev. B* **76**, 201304 (2007).
- [17] M. Grayson, L. Steinke, M. Huber, D. Schuh, M. Bichler, and G. Abstreiter, "Sharp quantum hall edges: Experimental realizations of edge states without incompressible strips," *Phys. Status Solidi (b)* **245**, 356 (2008).
- [18] L. Steinke, D. Schuh, M. Bichler, G. Abstreiter, and M. Grayson, "Hopping conduction in strongly insulating states of a diffusive bent quantum hall junction," *Phys. Rev. B* **77**, 235319 (2008).
- [19] M. Diez, I. C. Fulga, D. I. Pikulin, J. Tworzydło, and C. W. J. Beenakker, "Bimodal conductance distribution of Kitaev edge modes in topological superconductors," *New Journal of Physics* **16**, 063049 (2014).
- [20] D. S. Antonenko, E. Khalaf, P. M. Ostrovsky, and M. A. Skvortsov, "Mesoscopic conductance fluctuations and noise in disordered majorana wires," *Phys. Rev. B* **102**, 195152 (2020).
- [21] A. Yu. Kitaev, "Unpaired Majorana fermions in quantum wires," *Physics-Uspekhi* **44**, 131 (2001).
- [22] Y. Oreg, G. Refael, and F. von Oppen, "Helical liquids and majorana bound states in quantum wires," *Phys. Rev. Lett.* **105**, 177002 (2010).
- [23] C. W. J. Beenakker, "Search for Majorana fermions in superconductors," *Annu. Rev. Condens. Matter Phys.* **4**, 113 (2013).
- [24] I. A. Gruzberg, N. Read, and S. Vishveshwara, "Localization in disordered superconducting wires with broken spin-rotation symmetry," *Phys. Rev. B* **71**, 245124 (2005).
- [25] K. Efetov, *Supersymmetry in disorder and chaos* (Cambridge University Press, 1999).
- [26] M. R. Zirnbauer, "Fourier analysis on a hyperbolic supermanifold with constant curvature," *Comm. Math. Phys.* **141**, 503 (1991).
- [27] M. R. Zirnbauer, "Super Fourier analysis and localization in disordered wires," *Phys. Rev. Lett.* **69**, 1584 (1992).
- [28] M. Bocquet, D. Serban, and M. R. Zirnbauer, "Disordered 2d quasiparticles in class D: Dirac fermions with random mass, and dirty superconductors," *Nucl. Phys. B* **578**, 628 (2000).
- [29] E. Khalaf, *PhD Thesis "Mesoscopic Phenomena in Topological Insulators, Superconductors and Semimetals"* (Stuttgart, 2016).
- [30] I. A. Gruzberg, A. D. Mirlin, and M. R. Zirnbauer, "Classification and symmetry properties of scaling dimensions at anderson transitions," *Phys. Rev. B* **87**, 125144 (2013).
- [31] N. Read and A. W. W. Ludwig, "Absence of a metallic phase in random-bond Ising models in two dimensions: Applications to disordered superconductors and paired quantum hall states," *Phys. Rev. B* **63**, 024404 (2000).
- [32] A. D. Mirlin, A. Mullergroeling, and M. R. Zirnbauer, "Conductance fluctuations of disordered wires: Fourier analysis on supersymmetric spaces," *Ann. Phys.* **236**, 325 (1994).
- [33] S. Helgason, *Groups and Geometric Analysis. Integral Geometry, Invariant Differential Operators, and Spherical Functions*, Mathematical Surveys and Monographs, Vol. 83 (American Mathematical Society, 2000).
- [34] K. B. Efetov and A. I. Larkin, "Kinetics of a quantum particle in a long metallic wire," *Zh. Eksp. Teor. Fiz.* **85**, 764 (1983) [*Sov. Phys. JETP* **58**, 444 (1983)].
- [35] E. Khalaf and P. M. Ostrovsky, "Localization effects on magnetotransport of a disordered Weyl semimetal," *Phys. Rev. Lett.* **119**, 106601 (2017).
- [36] P. A. Lee and A. D. Stone, "Universal conductance fluctuations in metals," *Phys. Rev. Lett.* **55**, 1622 (1985).
- [37] M. C. W. van Rossum, I. V. Lerner, B. L. Altshuler, and T. M. Nieuwenhuizen, "Deviations from the gaussian distribution of mesoscopic conductance fluctuations," *Phys.*

- Rev. B **55**, 4710 (1997).
- [38] O. N. Dorokhov, “Transmission coefficient and the localization length of an electron in N bound disordered chains,” *Pis'ma v Zh. Eksp. Teor. Fiz.* **36**, 259 (1982) [*Sov. Phys. JETP Lett.* **36**, 318 (1982)].
- [39] B. Dutta, J. T. Peltonen, D. S. Antonenko, M. Meschke, M. A. Skvortsov, B. Kubala, J. König, C. B. Winkelmann, H. Courtois, and J. P. Pekola, “Thermal conductance of a single-electron transistor,” *Phys. Rev. Lett.* **119**, 077701 (2017).
- [40] A. V. Bubis, E. V. Shpagina, A. G. Nasibulin, and V. S. Khrapai, “Thermal conductance and nonequilibrium superconductivity in a diffusive nsn wire probed by shot noise,” *Phys. Rev. B* **104**, 125409 (2021).